Development of a space spectropolarimeter for full Stokes parameters retrieval

Bogdan Vasilescu[a], Yaël Nazé[b], and Jérôme Loicq[a]

[a]Université de Liège, Centre Spatial de Liège, Avenue du Pré Aily, Liège, Belgiume, 4031
[b]FNRS Senior Researcher, Université de Liège, Allée du Six Août, 19C, Liège, Belgium, 4000

ABSTRACT

This paper presents recent advancements in the study of a new concept of space spectropolarimeter. The instrument, based on a triple prismatic structure from a birefringent material, avoids the need of rotating components and may cover the entire Stokes vector for a very broad wavelength band. The analysis of the concept in noise-free conditions has proved its consistency. Further simulations for different geometries of the modulator are presented. The results allow identifying critical values for the main parameters. Moreover, the previous analysis of the instrument in noisy conditions is completed with the impact study of the spectral resolution, dimension of pixels and signal to noise ratio.

Keywords: polarization, spectropolarimetry, birefringence, modulation scheme, imaging spectropolarimetry

1. INTRODUCTION

The polarization is carrying essential information about the medium where the light originates or about the environment encountered on its path. In astronomy, for instance, it can be used to evaluate the magnetic field of stars, the distribution of interstellar medium or to characterize the surface of remote objects. Moreover, during the last years, polarimetry has also evolved into a method for the detection and study of exoplanets.[1–3] Nevertheless, the applications are going far beyond astronomy. Chemistry, biology, medicine are just a few domains that are making largely use of polarization today.

Two significant families of measurement techniques have been developed to determine the polarization of light: one using rotating components and another using amplitude division. However, both measurement procedures occupy a relatively large volume and make use of complex mechanisms. The considerable dimensions and the need for rotating parts are the most significant drawbacks for the space usage of these classical types of polarimeters. Indeed, they directly impact the cost, the design, and the reliability of space missions.

In this context, the method proposed by Pertenais and Sparks[4–6] and further developed by Vasilescu et al.,[7] for single-shot full Stokes polarimetry, has the advantage of being extremely compact and robust, without any moving components. The working principle is based on the modulation of the incoming signal due to the chromatic birefringence of the modulator, $\Delta n(\lambda)$, and to the geometry of the device.[4,8] Any incoming polarization state acquires a continuous modulation on vertical direction. The modulation is also wavelength dependent.

In our recent study,[7] the unicity of the solution for such instrument was demonstrated and the behaviour in noisy conditions was analyzed. It was also proved that a remarkably high polarimetric efficiency characterizes certain geometries. In a more realistic approach, the relative error on the degree of polarization and on the Stokes parameters is analyzed here for different geometries of the modulator, different integration steps and levels of noise. Recommendations for the architecture of the modulator can be inferred and the critical parameters are pointed out.

Further author information: (Send correspondence to Bogdan Vasilescu)
Bogdan Vasilescu: E-mail: bvasilescu@uliege.be

2. THE STATIC SPECTROPOLARIMETER CONCEPT

The new modulator uses three birefringent uniaxial elements made of the same material. For instance, the Magnesium Fluoride (MgF_2) or Calcium Fluoride (CaF_2) may ensure both the coverage of a large spectral band and they have a very well known refractive index. Nevertheless, the Magnesium Fluoride is more reliable from the point of view of manufacturing. Because of this, our simulations are based on the birefringence of MgF_2. Two anti-parallel wedges, (parts (1) and (3) in Fig. 1), of very small apex angles, ξ, and ψ, are optically glued together with the help of a third piece placed in between (element (2)). The fast axis has a specific orientation in each component of the modulator: parallel to the x-axis in the first wedge, parallel to z-axis in the middle part and at 45° with regard to x-axis (in the (xy) plane) in the last wedge.

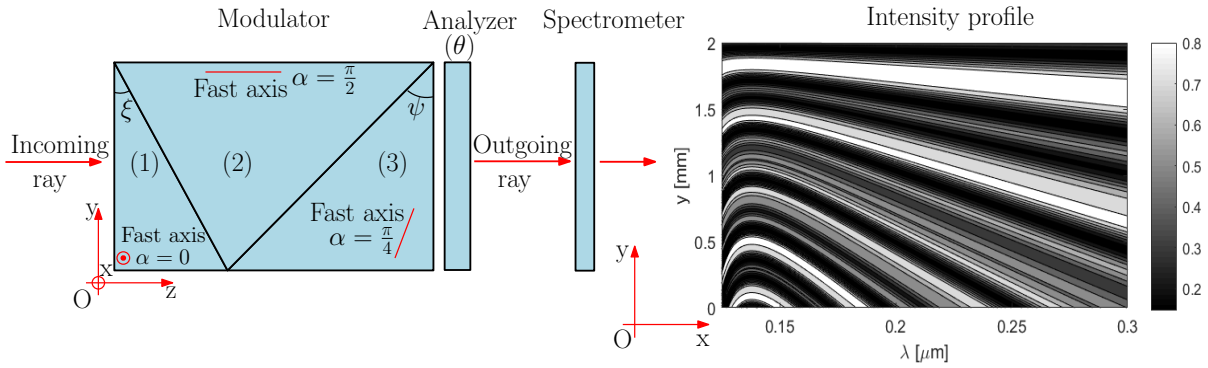

Figure 1. The incoming light arriving from the left-hand side is collimated and perpendicular to the surface of the instrument, the $(xy$ plane). After passing through the polarimeter, the emerging light has an intensity modulated along the vertical direction (along the y-axis). The spectrometer then leads to a wavelength dispersion along the horizontal direction (x-axis). The observed intensity profile represented here corresponds to an arbitrary state of polarization $\mathbf{S} = [1, 0.4, 0.3, 0.5]^T$ and to a modulator build in MgF_2, with the apex angles $\xi = 1.5°$ and $\psi = 3°$. The orientation of the analyzer was $\theta = 90°$. Additionally, it was considered that the entire incoming beam is identically polarized, being characterized by a single polarization state, i.e. the vector $\mathbf{S}$.

Aside from the modulator, the polarimeter uses an analyzer oriented at an angle θ about the x axis, in the plane (xy). After the passage through the polarimeter, the light is spectrally dispersed by the spectrometer over the x-axis.

Using the Stokes formalism, that describes the polarization with the help of a vector with four parameters, ($\mathbf{S} = [I, Q, U, V]^T$), and the Mueller calculus, the light passing through this modulator receives a modulation expressed as:

$$I_{out}(\theta, y, \lambda) = \frac{1}{2}(I_{in} + Q_{in} \cdot m(\theta, y, \lambda) + U_{in} \cdot n(\theta, y, \lambda) + V_{in} \cdot p(\theta, y, \lambda)) \,, \tag{1}$$

where

$$\begin{cases} m(\theta, y, \lambda) = \cos(2\theta) \cos \Delta\phi_3 \\ n(\theta, y, \lambda) = \sin(2\theta) \cos \Delta\phi_1 + \cos(2\theta) \sin \Delta\phi_1 \sin \Delta\phi_3 \\ p(\theta, y, \lambda) = \cos(2\theta) \cos \Delta\phi_1 \sin \Delta\phi_3 - \sin(2\theta) \sin \Delta\phi_1 \end{cases} \tag{2}$$

and

$$\begin{cases} \Delta\phi_1 = \frac{2\pi}{\lambda} \Delta n(\lambda)(h - y) \tan \xi \\ \Delta\phi_3 = \frac{2\pi}{\lambda} \Delta n(\lambda)(h - y) \tan \psi, \end{cases} \tag{3}$$

where $\Delta n(\lambda) = |n_o(\lambda) - n_e(\lambda)|$ is the birefringence of the material, and $\mathbf{S_{in}} = [I_{in}, Q_{in}, U_{in}, V_{in}]^T$ is the incoming Stokes vector.

Fitting the function (1) with the data from the detector plane, the Stokes parameters can be inferred.

3. METHOD

The precision of measurements with this type of instrument is directly affected by the incoming Stokes vector, the orientation of the analyzer (the angle θ in Fig.1), the geometry of the modulator (the angles ξ and ψ), the dimension of pixels on vertical direction, by the spectral resolution (R), and the signal to noise ratio (SNR). In order to account for all these parameters and also for the incoming Stokes vector, a series of simulations were conducted for different configurations and a large number of incoming polarizations, randomly generated. Then, the degree of polarization, defined by

$$p = \frac{\sqrt{Q^2 + U^2 + V^2}}{I}. \tag{4}$$

was calculated, together with the corresponding relative error

$$\frac{\Delta p}{p} = \frac{|p_m - p_0|}{p_0}. \tag{5}$$

The same procedure was applied for the Stokes parameters individually.

4. THE GEOMETRY OF THE MODULATOR

The most important parameters of the modulator are the apex angles ξ and ψ of the two opposite prisms. They directly affect the phase difference induced by the modulator (Eq. 3) and consequently the shape of the functions $m(\theta, y, \lambda), n(\theta, y, \lambda)$ and $p(\theta, y, \lambda)$ (Eq. 2). Therefore, they translate into the modulation of the signal (Eq. 1).

The ratio between the uncertainty characterizing the retrieval of the Stokes parameters and uncertainty corresponding to the detected intensity was mapped in Vasilescu et al.,[7] for two different apex values of the modulator and all the possible orientations of the analyzer. The least-square fit method was previously used under the assumption of Gaussian noise. The relative error corresponding to the measurement of a given state of polarization is further analyzed. This time the analysis is extended simultaneously to all possible apex angles of the opposite prisms of the modulator, comprised between 1° and 3°. The purpose is to map the behaviour of the instrument for different geometries so that the best choice for the construction to become accessible.

Because the values of the Stokes parameters also influence the fitting process, a Monte Carlo approach was used and 100 random values of the Stokes vector were generated. For each of these values, the impact of the geometry of the modulator was then calculated with the help of the relative error on the degree of polarization and on Stokes parameters. In the end, the mean value of the errors was plotted.

Therefore, in Fig. 2 (a,b) we observe the behaviour of the relative error on the degree of polarization as a function of ξ and ψ angles, for two orientations of the analyzer: $\theta = 32.5°$ and $\theta = 50.6°$. The values of the SNR and of the spectral resolution (R) were chosen so that the corresponding error to be negligible.

As it can be noticed from the Fig. 2 (a,b), equal values of the apex angles are accompanied by the highest error in the measurement of polarization. The phenomenon is due to the fact that the functions $n(\theta, y, \lambda)$ and $p(\theta, y, \lambda)$ are becoming very close to each other for this particular values. Consequently, the pattern of the intensity does not allow a proper determination of all the Stokes parameters.

Nevertheless, the orientation of the analyzer plays an important role in any configuration of the angles ξ and ψ. Therefore, even for $\xi = \psi$ there exist orientations of the analyzer able to mitigate the error on the degree of polarization.

From the Fig. 2 (c) we observe that for $\theta = 32.5°$ or $\theta = 116.3°$ the error on the degree of polarization is at minimum. Observing with the same configuration of apex angles at $\theta = 50.6°$ we reach a maximum of relative

error on the degree of polarization (Fig. 2 (c)). Overall, the relative error on the Stokes parameters remains at a height level for these precise values of ξ and ψ, especially for Q and U.

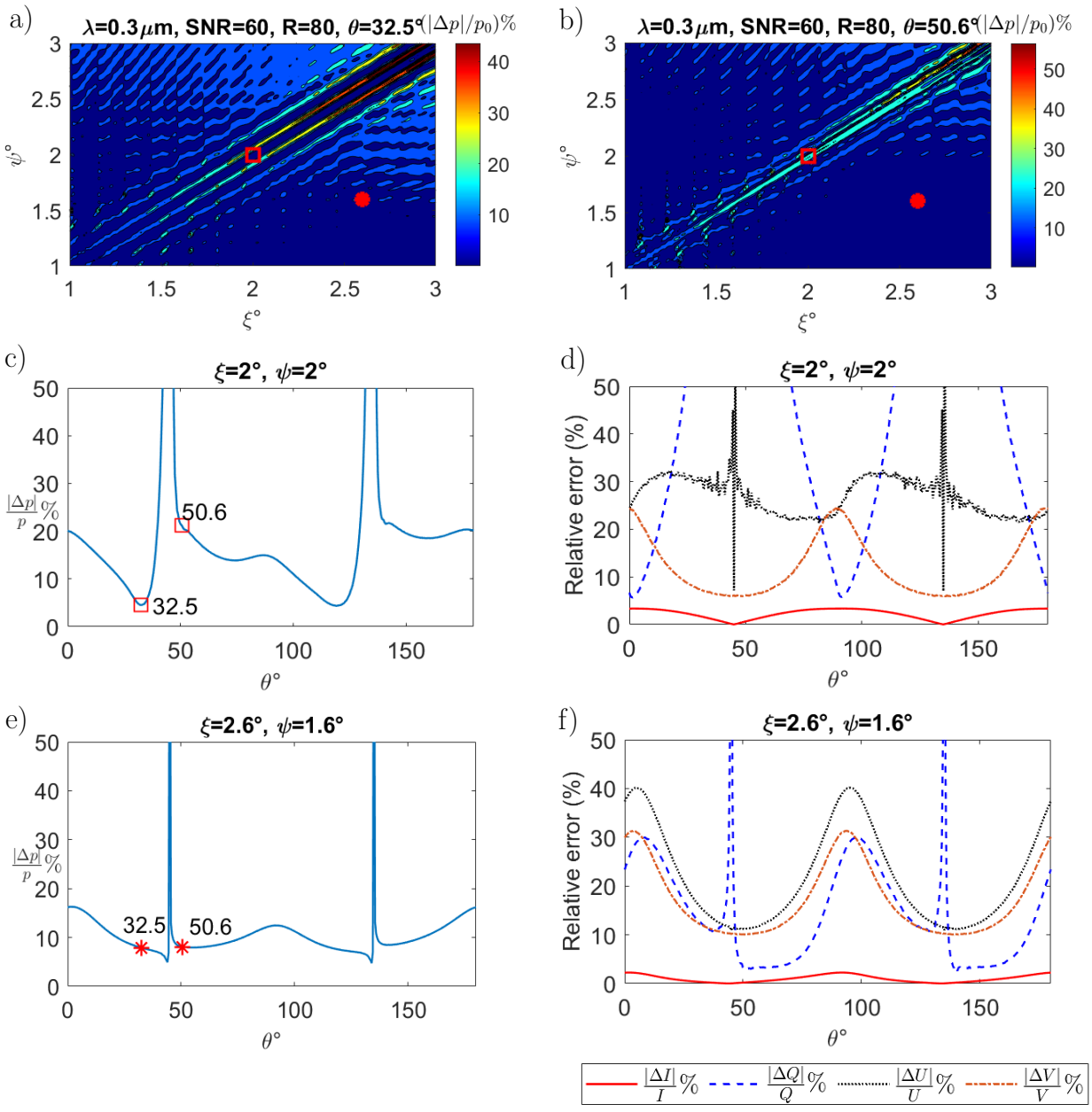

Figure 2. Detailed view of the impact of the angles ξ and ψ of the two opposite wedges of the modulator. For 200 values of these angles, spanning from 1° until 3°, the relative error characterising the measured degree of polarization for a given incoming vector was calculated. An $SNR = 60$, a spectral resolution $R = 80$, and a pixel size $\Delta y = 15\,\mu$m were considered in order to simplify the graphical interpretation. The input was represented by 100 Stokes vectors arbitrary generated as a Monte Carlo approach. In the end, the mean value of the relative error was represented for the degree of polarization and for Stokes parameters.

For a different configuration of the apex angles, (i.e. $\xi = 2.6°$, $\psi = 1.6°$), chosen from the region of low error it can be noticed that the orientation of the analyzer has a limited impact over the measured degree of polarization

(Fig. 2-e). Also, the error on the Stokes parameters individually remains at a lower level, with almost the same behaviour for U and V with regard to the orientation of the analyzer (Fig. 2-f).

5. SOURCES OF ERRORS

Our previous research has addressed the issue of noise in order to assess the uncertainties and the efficiency of the modulation scheme.[7] The approach allowed to understand the limitations of the system and the behaviour of the functions $m(\theta, y, \lambda), n(\theta, y, \lambda), p(\theta, y, \lambda)$, responsible for the polarimetric modulation.

Nevertheless, aside from the shot noise, considered before, the demodulation process is also affected by the pixel size (on vertical direction), by the spectral resolution (R), and the level of noise, generally considered through the signal to noise ratio (SNR). The pixel size (on the vertical direction) and the spectral resolution directly affect the integration of the signal as they are variables in the modulation function (Eq. 1). The SNR affects the fitting quality of the experimental data with the theoretical curve.

A series of simulations were conducted in order to assess the impact of these three parameters.

Therefore, from Fig. 3-a) we may notice that the variation of the pixel size, in the limits of the Nyquist theory, has a small impact on the quality of measurements, whereas the SNR plays a major role. This behaviour may be also easily observed with the help of Poincaré spheres (Fig. 3-c). At low SNR, the retrieved polarization spans on a large area around the incoming state of polarization, with deviations in the values of the Stokes parameters and also of the degree of polarization. Higher is the SNR, lower becomes the difference between the relative error on the Stokes parameters, as suggested by the Fig. 2, for $\theta = 32.5°$, and $\xi = 2.6°$, $\psi = 1.6°$. For this simulation 100 measurements of the same incoming vector, $\mathbf{S} = [1, 0.5, 0.5, -0.1]^T$, were considered in order to take into account the random distribution of noise.

The spectral resolution is also a key factor for the precision of measurements given the fact that the modulation is wavelength dependent. At small R, even for high values of the SNR, the relative error on the degree of polarization stays around 5% (Fig. 3-b).

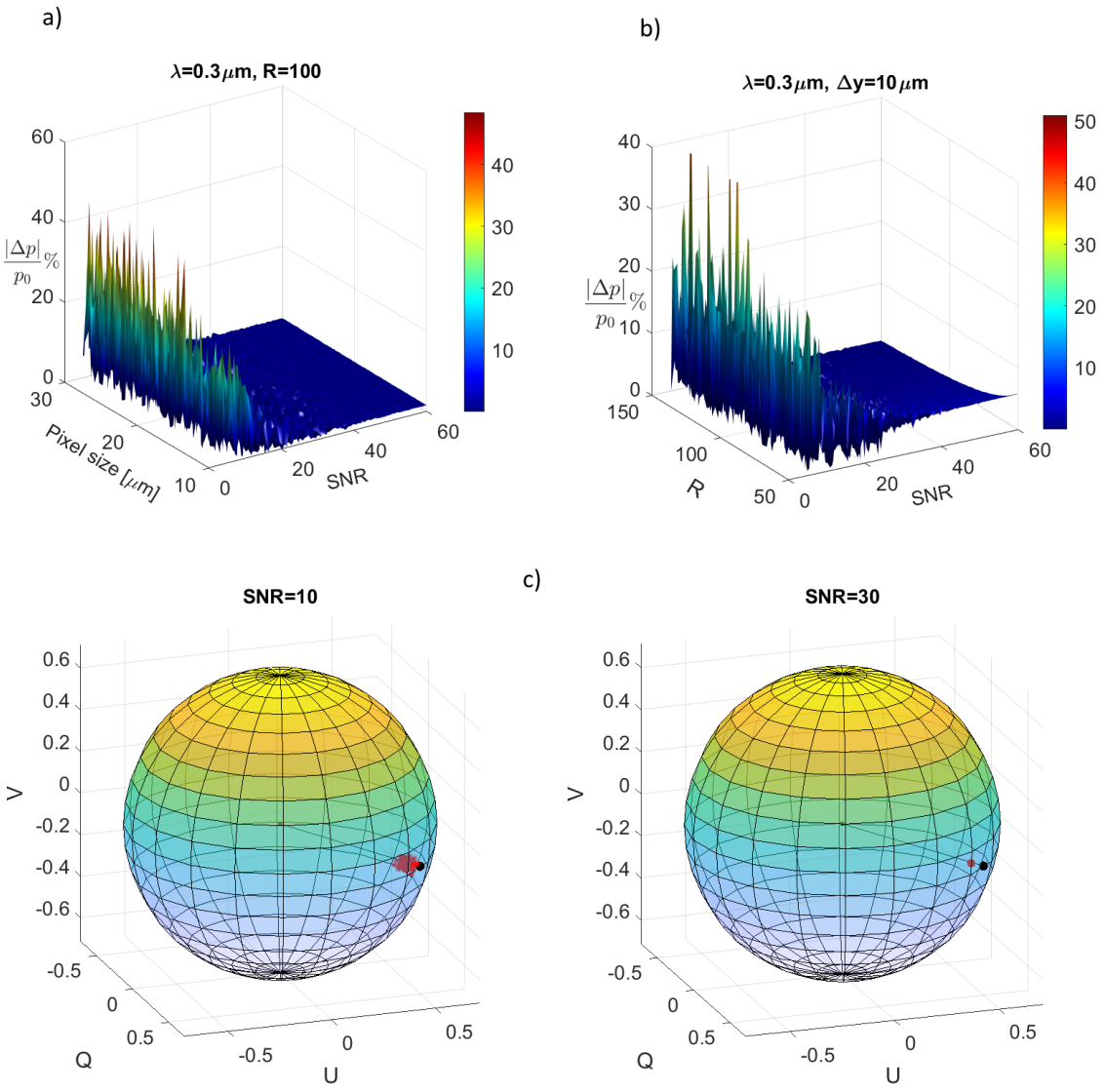

Figure 3. Relative error on the measurement of the degree of polarization as a function of the pixel size and signal to noise ratio (SNR) (a), and as a function of SNR and spectral resolution (R). The Poincaré representation is provided for two different values of SNR, a pixel size of $10\mu m$ and a spectral resolution, $R = 50$. The black dot represents the incoming S vector, and the red dots are the measured Stokes vectors. For each sphere, 100 simulations (red dots) were randomly generated to take into account the Gaussian noise. For these simulations, a modulator having $\xi = 2.6°$ and $\psi = 1.6°$ was considered. The angle of the analyser is $\theta = 32.5°$. and the incoming Stokes vector, $\mathbf{S} = [1, 0.5, 0.5, -0.1]^T$.

6. CONCLUSIONS

The orientation of the analyzer can mitigate the error on the degree of polarization and even on a part of the Stokes parameters, but the minimum, the maximum level as well as the differences between the Stokes parameters are dictated by the apex angles of the two opposite prisms of the modulator. The configurations for which the relative error is highly dependent on the orientation of the analyzer are those with equal values of ξ and ψ, or very close one to another. Even if for this geometries can be found orientations of the analyzer able to drastically diminish the error on the degree of polarization, the disparities between the errors on the Stokes parameters remains high at these orientations.

The configurations with large ξ angle and small ψ (or small ξ and large ψ) are proved to be more independent on the orientation of the analyzer and with relatively close errors on the Stokes parameters.

From the point of view of the noise and sources of errors, aside the level of the SNR, the spectral resolution is proved to be the factor with the highest impact on the quality of the measurements. The pixel size plays a limited role in the precision of measurements, as long as it stays below the Nyquist limit.

REFERENCES

[1] Bailey, J., Kedziora-Chudczer, L., and Bott, K., "Polarized radiative transfer in planetary atmospheres and the polarization of exoplanets," *Mon. Not. R. Astron. Soc.* **480**(2), 1613–1625 (2018).

[2] Rossi, L. C. G. and Stam, D. M., "Circular polarization signals of cloudy (exo)planets," *Astron. Astrophys.* **616**, A117 (2018).

[3] Kolokolova, L., Hough, J., and Levasseur-Regourd, A. C., [*Polarimetry of Stars and Planetary Systems*], Cambridge University Press (2015).

[4] Pertenais, M., Neiner, C., Bernardi, P., Reess, J.-M., and Petit, P., "Static spectropolarimeter concept adapted to space conditions and wide spectrum constraints," *Appl. Opt.* **54**, 7377–7386 (Aug 2015). [doi:10.1364/AO.54.007377].

[5] Pertenais, M., *Spectropolarimétrie stellaire UV et visible depuis l'espace*, PhD thesis, Université Toulouse III - Paul Sabatier (2016).

[6] William, S., Thomas, G. A., MacKenty, J. W., and Snik, F., "Compact and robust method for full Stokes spectropolarimetry," *Appl. Opt.* **51**, 5495–5511 (Aug 2012). [doi:10.1364/AO.51.005495].

[7] Vasilescu, B., Nazè, Y., and Loicq, J., "Solution uniqueness and noise impact in a static spectropolarimeter based on birefringent prisms for full Stokes parameter retrieval," *J. Astron. Telesc. Instrum. Syst.* **6**, 1 (Apr. 2020). [doi:10.1117/1.JATIS.6.2.028001].

[8] Pertenais, M., Neiner, C., Parès, L. P., Petit, P., Snik, F., and van Harten, G., "UVMag: Space UV and visible spectropolarimetry," in [*Space Telescopes and Instrumentation 2014: Ultraviolet to Gamma Ray*], Tadayuki, T., den Herder, J.-W. A., and Bautz, M., eds., *Proc. SPIE* **9144**, 1017–1025 (2014). [doi:10.1117/12.2060561].